Numerical Model for the Minimization of Intermixed Round Bars in a Four Line Continuous Caster

MARCELA B. GOLDSCHMIT, SERGIO P. FERRO, GUILLERMO F. WALTER, VIRGINIA G. ARANDA, and JORGE A. TENA MORELOS

The grade transition process in a four line round billets continuous caster was analyzed. A numerical model was developed to determine, quickly and accurately, the length and location of intermixed steel in the bar. The model is based on "tank in series" or "volumes" mathematical models and was calibrated with physical water model measurements and full three-dimensional (3-D) turbulent numerical calculations. Comparison of the model with measurements performed on intermixed steel bars is also presented. The good agreement between these plant measurements and the numerical results validated the model. The model was implemented on PCs with a visual interface that allowed the easy input and output of data, and the program is operated in a steel shop. Finally, the code was employed to evaluate different strategies to fill the tundish during grade transitions. The "double dilution" process, which consists of filling the tundish in two steps, proved to be useful to reduce the amount of downgraded steel.

I. INTRODUCTION

SEQUENTIAL casting of different steel grades during the continuous casting process is often employed in steel plants in order to maximize the productivity of the caster. This procedure, however, generates an amount of mixed steel that does not satisfy the required specifications and must be downgraded. The motivation of the present work is to develop a numerical model of the chemical composition of the steel bars during a grade transition and to provide an estimation of the position and length of the bars of intermixed steel.

Transition grade models[1–6] have been published in the literature since 1992. Numerical models, physical water models, and experimental studies were employed to address the problem. Most publications have considered grade transitions with only two continuous casting lines. Casters with more than two lines have received much less attention in the literature.[7]

Several publications[1,8,9] on grade transition models have focused on mixing in the tundish. Diener *et al.*[10] incorporated the mixing in the mold into the transition models, while Huang and Thomas[2] included mixing in the strand.

Several studies[1–10] developed grade transition models with "tank in series" mathematical models, also called "box models" or "volume models." All these models, however, consider a one-step filling of the tundish, with the tundish volume increasing monotonically until its operating value.

The aim of this work is to develop a numerical model that can predict the location of the intermixed steel in a four line round caster, quickly and accurately, for a wide variety of casting conditions, including time-dependent casting speed and time-dependent inlet flow rate. This model could be used to optimize the casting conditions during a grade change, to find the best sequence of grades to be cast, and to specify the points where the bars should be cut. All these improvements tend to reduce the intermix costs when different grades are cast in single sequence. By estimating these costs, the model also helps to decide when a tundish change is convenient. The model focuses on the four line round billet caster used at Siderca, but it can be easily modified for other applications.

This model consists of three submodels: one associated with the tundish, which was tested and calibrated with water model measurements performed by IAS;[11] a second one associated with the mold and upper part of the bar, which was calibrated with a three-dimensional (3-D) numerical k-ε turbulent model using a (k-L)-predictor/(ε)-corrector iterative algorithm (this turbulent model was addressed in our previous publications[12,13] and was used to model the liquid steel flow in submerged entry nozzles, round molds, and slab molds[14,15,16]); and the last submodel associated with the final composition in the bar, which solves a convection-diffusion equation (with the turbulent diffusivity estimated by the 3-D model). The model was implemented in our user friendly code GRADE.[21]

The description of the model is presented in detail in sections II through IV. In Section V, plant measurements of intermixed steel composition made in the SIDERCA Steel plant, which validate the numerical model, are shown. Different dilution strategies of two steel grades are shown in Section VI. In Section VII, possible extensions of the model to caster with any number of lines are discussed. The last Section is devoted to the conclusions.

II. MODELING CRITERIA

An important point to keep in mind is that, as the flow is highly turbulent, the turbulent diffusivity is much greater than the molecular one. Consequently, all chemical species will show the same behavior. This was confirmed by plant

MARCELA B. GOLDSCHMIT, Head of Computational Mechanics Department, and SERGIO P. FERRO, Researcher, are with the Center for Industrial Research (CINI), Fundación para el Desarrollo Tecnológico (FUDETEC)-Córdoba 320, 1054 Buenos Aires, Argentina. GUILLERMO F. WALTER, Head of Continuous Casting Department, VIRGINIA G. ARANDA, Steelmaking Process Assistant, and JORGE A. TENA MORELOS, Manufacturing Director Assistant, Siderca S.A.I.C., Av. Simini 250, 2804 Campana, Argentina.

Manuscript submitted July 28, 2000.

Table I. Description of the Basic Volumes

Equation	Mixing Volume (V_m)	Dead Volume (V_d)	Plug Volume (V_p)
	$\xrightarrow[C_{in}]{Q^{in}}$ [V_m] $\xrightarrow[C_{our}]{Q^{out}}$	$\xleftrightarrow[C]{Q}$ [V_d]	$\xrightarrow[C_{in}]{Q^{in}}$ [V_p] $\xrightarrow[C_{out}]{Q^{out}}$
Mass conservation	$\frac{dV_m}{dt} = Q_{out} - Q_{in}$	$\frac{dV_d}{dt} = \pm Q$	$\frac{dV_p}{dt} = Q_{out} - Q_{in}$
Mass conservation of a chemical elements	$\frac{dC_{out}}{dt} = \frac{Q_{in}}{V_{in}}(C_{in} - C_{out})$	$C \neq f(Q,V)$	$C_{out} = C_{in}\left(t - \frac{V_p}{Q_{in}}\right)$

measurements described in Section V. Thus, concentration calculations were performed for a single dimensionless function ($\tilde{C}(t)$) defined by

$$\tilde{C}(t) = \frac{C(t) - C_{old}}{C_{new} - C_{old}} \quad [1]$$

where C_{old} and C_{new} represent the concentration of a given element in the old and new steel grade, respectively. This dimensionless concentration can take any value between 0 (old steel grade) and 1 (new steel grade). Once the dimensionless concentration is calculated, the concentration of a given chemical element ($C(t)$) may be obtained from Eq. [1].

The model is composed of three types of volumes: mixing volume, dead volume, and plug volume. The basic equations of the model may be derived by imposing mass conservation for the fluid and for the chemical elements in each volume. Mixing volumes are assumed to be well mixed, having a uniform concentration equal to the outgoing one for each time interval. Plug flow volumes introduce a delay (t_p) in the outgoing concentration. Table I provides the descriptions and the equations for the three volumes.

The time $t = 0$ is considered when the ladle with the new steel grade is opened.

The model consists of three submodels: tundish, mold, and final composition.

III. TUNDISH MIXING MODEL

A. *Volumes Model*

The flow inside the tundish was modeled by a tank in series mathematical model. Several "tanks" or "volumes" were considered to model a four line symmetric tundish with isothermal flow. In Figure 1, we show the mixing volume model of half the tundish with the internal and external continuous casting lines.

There are two well-defined groups of volumes: one of them associated with the internal lines (superscript int) and the other associated with the external lines (superscript ext), with an extra recirculating mixing volume (V_m^R), which allows the mass flow between both groups of volumes.

Each of these groups consists of two mixing volumes (V_{m1} and V_{m2}), one dead volume (V_d), and one plug flow volume (V_p).

B. *Equations*

Using the basic equations previously described in Table I and assembling them according to Figure 1, we reach the following system of equations,

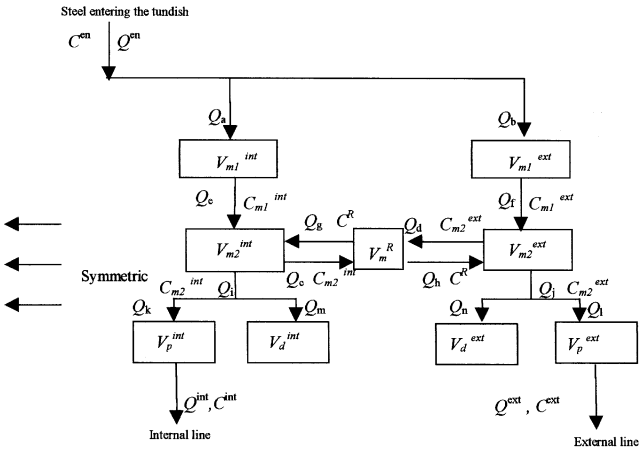

Fig. 1—Tundish mixing model.

$$Q_a = x_a Q^{en} \qquad Q_b = Q^{en} - Q_a$$
$$Q_e = Q_a - dV_{ml}^{int}/dt \qquad Q_f = Q_b - dV_{ml}^{ext}/dt$$
$$Q_k = Q^{int} + dV_p^{int}/dt \qquad Q_l = Q^{ext} + dV_p^{ext}/dt$$
$$Q_m = dV_d^{int}/dt \qquad Q_n = dV_d^{ext}/dt$$
$$Q_i = Q_k + Q_m \qquad Q_j = Q_l + Q_n$$
$$Q_c = x_c Q_i \qquad Q_d = x_d Q_j$$
$$Q_g = Q_c + Q_i - Q_e + dV_{m2}^{int}/dt \quad [2]$$
$$Q_h = Q_d + Q_j - Q_f + dV_{m2}^{ext}/dt$$
$$C^{int} = C_{m2}^{int}(t - t_p^{int}) \qquad C^{ext} = C_{m2}^{ext}(t - t_p^{ext})$$
$$dC_{ml}^{int}/dt = Q_a(C^{en} - C_{ml}^{int})/V_{ml}^{int}$$
$$dC_{ml}^{ext}/dt = Q_b(C^{en} - C_{ml}^{ext})/V_{ml}^{ext}$$
$$dC_{m2}^{int}/dt = (Q_e C_{ml}^{int} + Q_g C^R - (Q_g + Q_e)\, C_{m2}^{int})/V_{m2}^{int}$$
$$dC_{m2}^{ext}/dt = (Q_f C_{ml}^{ext} + Q_h C^R - (Q_f + Q_h) C_{m2}^{int})/V_{m2}^{ext}$$
$$dC^R/dt = (Q_d C_{m2}^{ext} + Q_c C_{m2}^{int} - (Q_d + Q_e) C^R)/V_m^{ext}$$

In this system of equations, the volume fractions $f_i = V_i/V_T$ are parameters to be calibrated with the water model. The total flow rate entering (Q^{en}) and leaving ($Q^{int} + Q^{ext}$) the tundish are known functions of time, which the user must specify. Consequently, the half-tundish volume (V^T) is also a known function of time.

There are three flow rate fractions to be calibrated:

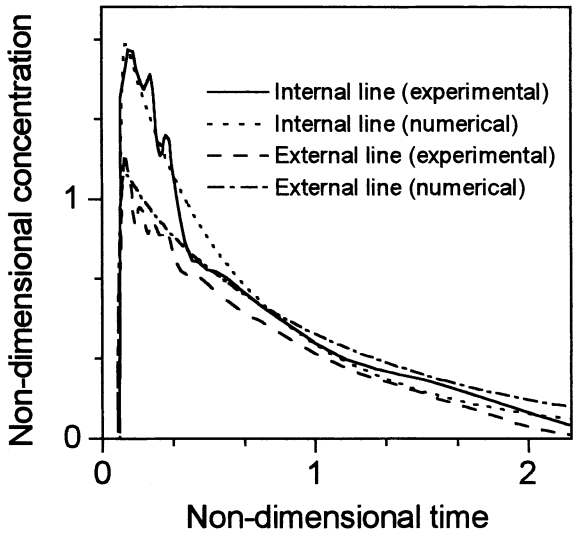

Fig. 2—Calibration of the tundish mixing model.

$x_a = \dfrac{Q_a}{Q_{en}}$ (fraction of entering flow rate directed to the internal line);

$x_d = \dfrac{Q_d}{Q_j}$ (fraction between the two flow rates coming out of V_{m2}^{ext}); and

$x_c = \dfrac{Q_c}{Q_i}$ (fraction between the two flow rates coming out of V_{m2}^{int}).

The new grade composition prescribes the concentration of the chemical elements at the tundish entrance, C^{en}. The time delay introduced by the plug flow volumes is given by $t_p^{\text{int}} = V_P^{\text{int}}/Q_k^{\text{int}}$ and $t_P^{\text{ext}} = V_P^{\text{ext}}/Q_l^{\text{ext}}$.

The system of coupled ordinary differential equations was solved with a fourth-order Runge Kutta algorithm, with the old grade composition as initial composition.

C. *Water Model Calibration*

The tundish model just described was calibrated with experimental measurements performed by IAS[11] on a physical water model. The water model is a 1:3 scale reproduction of the tundish at Siderca S.A.I.C. (Campana, Argentina), which is 14 tons in weight and is equipped with an impact pad. The experiment simulated a constant velocity of 2.1 m/min in each continuous casting line of bars with a diameter of 0.140 m.

The tracking of concentration was accomplished by injecting a salt solution into the tundish entrance and analyzing the flow coming out of each line for different time instants.

The residence time distribution (RTD) curves are presented in Figure 2. The time is represented in terms of the theoretical mean residence time $\hat{t} = tQ^e/V_T$, $t = 0$ being the moment when the salt solution was injected. The nondimensional concentration in Figure 2 was defined in such a way that the area beneath the innerline curve is unity, $\hat{C} = C/\int_0^\infty C(\hat{t})d\hat{t}$.

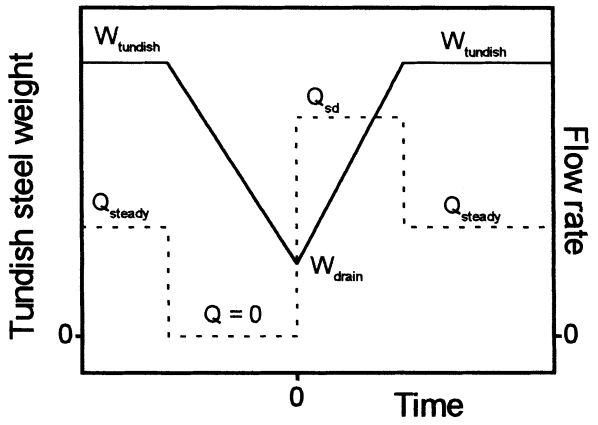

Fig. 3—Scheme of a simple dilution procedure. Full lines indicate the weight of the steel in tundish and dotted lines the flow rate of the steel entering the tundish.

To determine the group of parameters that best fits the RTD curves obtained by the water model experiment, the function $\sum_k (C_{\text{int}}(t_k) - C_{\text{int}}^{wm}(t_k))^2 + (C_{\text{ext}}(t_k) - C_{\text{ext}}^{wm}(t_k))^2$ was considered. In this expression, the superscript *wm* indicates concentrations obtained by the water model experience and t_k represents the time intervals when concentrations were evaluated. The parameter space was explored in order to find the set of parameters that minimizes this function.

The resulting parameters are as follows:

$$f_{ml}^{\text{ext}} = f_{ml}^{\text{int}} = 0.0004 \quad f_{m2}^{\text{int}} = 0.33 \quad f_{m2}^{\text{ext}} = 0.44$$
$$f^R = 0.08 \quad f_P{}^{\text{int}} = 0.04 \quad f_p^{\text{ext}} = 0.035 \qquad [3]$$
$$f_{dl}^{\text{ext}} = f_{d2}^{\text{int}} = 0.0371 \quad x_a = 0.53 \quad x_d = x_c = 0.36$$

The nondimensional concentrations obtained by setting these parameters in the numerical model are plotted in Figure 2.

D. *Simple and Double Dilution*

During normal operation, the steel weight in the tundish is kept almost constant at a certain value W_{tundish}. Under this condition, the flow rate entering the tundish Q_{steady} equals the flow rate leaving the tundish through its four lines. This flow rate is given by the casting speed and the bar diameter. When a ladle change takes place, no steel enters the tundish and the steel weight in the tundish is reduced to a minimum value W_{drain}. The filling of the tundish could be carried out in two different ways.

(1) *Simple dilution procedure*: When the new ladle opens, the flow rate entering the tundish is set to a value Q_{sd} above Q_{steady} until the operating weight W_{tundish} is reached. Then the caster is in normal operation again, with W_{tundish} and Q_{steady}. Figure 3 shows the time evolution of the weight of steel in the tundish and the inlet flow rate when a simple dilution procedure is adopted to fill the tundish.

(2) *Double dilution procedure*: The filling of the tundish is

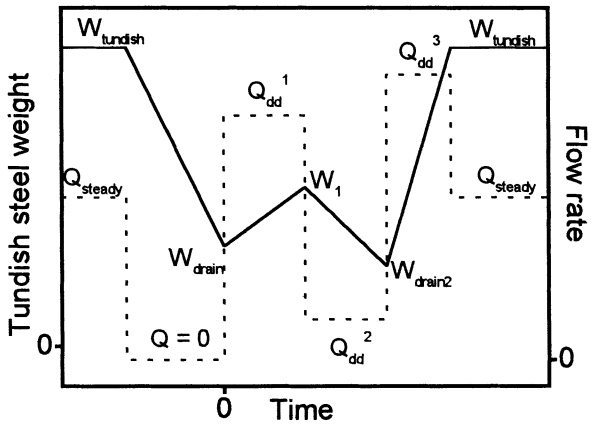

Fig. 4—Scheme of a double dilution procedure. Full lines indicate the weight of the steel in tundish and dotted lines the flow rate of the steel entering the tundish.

performed in two steps, as depicted in Figure 4. When the ladle with the new grade opens, it fills the tundish only up to a certain weight W_1 with a flow rate Q^1_{dd}. Then it closes for a while (in fact, it is not completely closed, a little flow rate Q^2_{dd} still entering the tundish), allowing for a second draining of the tundish. When a second minimum steel weight W_{drain2} is attained, the ladle opens with Q^3_{dd} flow rate, for the tundish to reach the operating weight W_{tundish}. Then the flow rate is reduced to the steady-state value Q_{steady}, in order to keep a constant steel weight in the tundish.

The time duration of each step is determined by the weight and the flow rate entering and leaving the tundish.

IV. MOLD MIXING MODEL AND FINAL COMPOSITION

A. *Volumes Model*

The model in the mold and upper part of the bars considers the first three meters of fluid below the meniscus. It was validated with a numerical full 3-D turbulence model[12–16] and consists of a plug flow volume and a mixing volume, followed by a region where convective and diffusive effects were supposed to take place (Figure 5). In this latter region, a one-dimensional convection (1-D) convection-diffusion equation was solved with the coordinate z (taken along the bar) being the only relevant variable.

The following set of equations for the concentration is obtained.

Mixing volume: [4]

$$\frac{dC_m}{dt} = \frac{Q}{V_m}(C_T - C_m)$$

Plug flow volume:

$$C_p = C_m\left(t - \frac{V_p}{Q}\right)$$

Convection-diffusion region:

$$\frac{\partial C_{Zf}}{\partial t} + v_z \frac{\partial C_{Zf}}{\partial z} = \frac{\partial}{\partial z}\left(D_{\text{eff}} \frac{\partial C_{zf}}{\partial z}\right); \quad z_i < z < z_f$$

where V_m is the mold mixing volume; V_p is the mold plug flow volume; C_m, C_p, and C_{Zf} are the concentrations exiting each region; v_z is the casting speed; D_{eff} is the turbulent diffusivity; $z_i = (V_m + V_p)/\pi\phi^2$ and z_f are the initial and final positions of the convection-diffusion region; and ϕ is the bar radius.

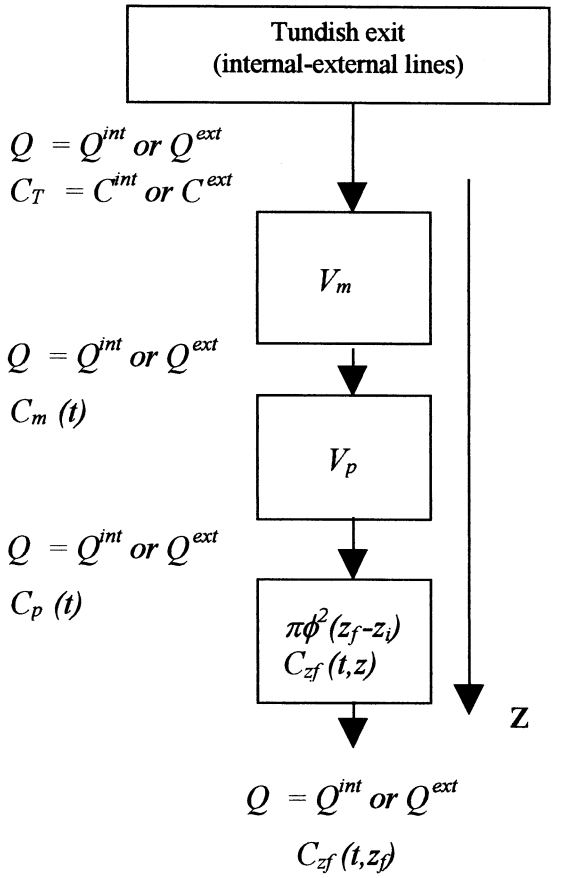

Fig. 5—Mold mixing model.

The values of Q and C_T are taken from the tundish mixing model, while the values of V_m, V_p, and D_{eff} are estimated by calibration with results obtained with a numerical 3-D turbulent model,[12–16] as described subsequently.

B. *Validation with a 3-D Finite Element Model*

The mold mixing model was calibrated in the following way.

(1) The steel flow inside the system nozzle-mold-bar was numerically calculated using a 3-D code.[17] This code solves the k-ε turbulent flow equation using a (k-L)-predictor/(ε)-corrector iterative algorithm. This was addressed in our previous publications.[12–16] These calculations were performed considering different casting speeds and mold diameters. The modeled domain includes the nozzle, the mold, and part of the bar to 3 m below the meniscus.

(2) Once the velocity field was obtained, the transport equation for a chemical element in a turbulent stream was calculated by solving a transient turbulent convection-diffusion equation:

$$\frac{\partial C}{\partial t} + \underline{v} \cdot \underline{\nabla} C = \underline{\nabla} \cdot [(D + D^t)\, \underline{\nabla}\, C] \qquad [5]$$

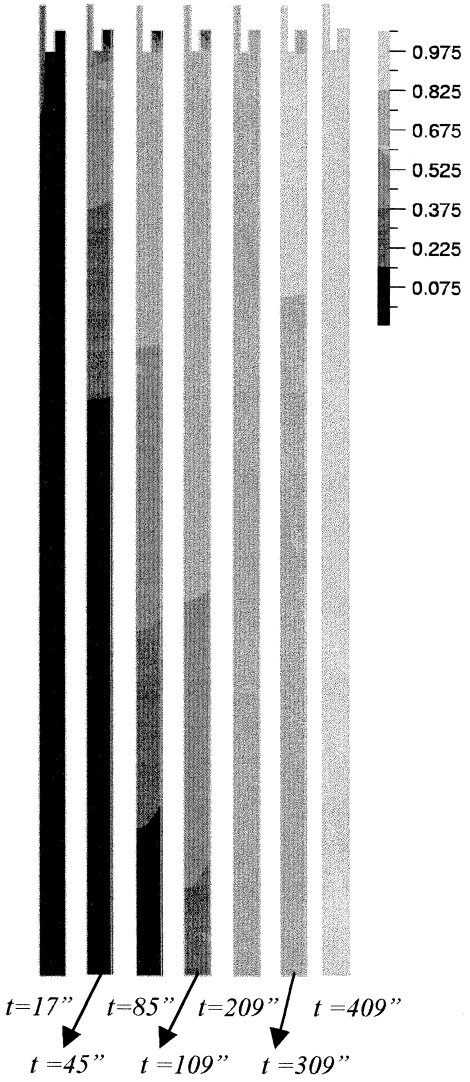

Fig. 6—Concentration in the system nozzle mold bar for different time instants.

where c is the time-averaged concentration for a chemical species; $\underline{v}$ is the time-averaged velocity; D is the molecular diffusivity for the species; and D^t is the turbulent diffusivity. The value of D^t was considered to be equal to the turbulent dynamic diffusivity $D^t = (\mu^t/\rho)$ (μ^t: turbulent viscosity given by the k-ε model, and ρ: density) and $D << D^t$. Therefore, all species have the same concentration distribution behavior.

Equation [5] is integrated with the Streamline Upwind Petrov Galerkin technique,[18,19] and a standard eight-node (3-D) isoparametric finite element discretization[20] for c.

Free parameters of the 1-D model were calibrated with the concentration obtained by these 3-D calculations. The following values were found:

$$V_m = \pi\phi^2 \times 0.5 \text{ m};$$

$$V_p = \pi\phi^2 \times 1.06 \text{ m; and}$$

$$D_{\text{eff}} \approx 30 \text{ mm}^2/\text{seg}$$

Figure 6 shows the external line dimensionless concentration distribution for different time intervals in the azimuthal plane. This figure was obtained in a simulation with a casting speed of 2 m/min and a mold diameter of 0.170 m. The concentration imposed at the nozzle was given by the tundish model, assuming a typical double dilution process.

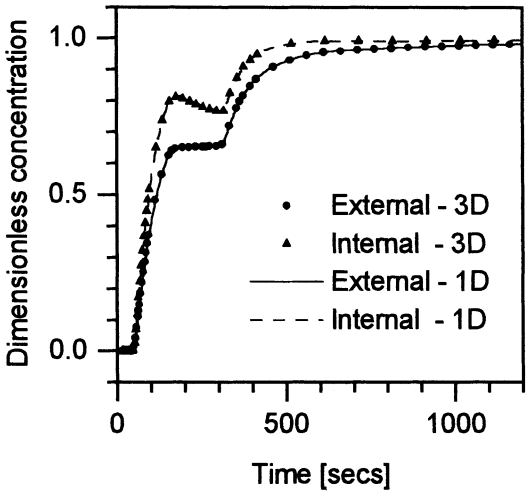

Fig. 7—Comparison of dimensionless concentration at 1.56 m below meniscus as given by the 1-D volumes model and the 3-D turbulent model.

Results from the 3-D numerical model show an almost 1-D flow below a distance of 1.5 m from the meniscus. In Figure 7, the dimensionless concentration at 1.56 m below the meniscus is plotted as a function of time. In this figure, lines correspond to 1-D model results and symbols to 3-D model results. The good agreement observed validates the use of the 1-D model. The abrupt slope change in both lines is due to the double dilution process already stated.

C. *Final Composition of the Bar*

The third submodel simulates the lower part of the liquid pool (from 1.56 m below the meniscus to the metallurgical length). It solves the convection diffusion equation (Eq. [5]) using the turbulent diffusivity given by the 3-D numerical model. Diffusion in solid state is neglected.

The solidification point would be different for each point of the bar cross section depending on its distance to the surface.

The complete solution of Eq. [5] proved that diffusive effects can also be neglected in the liquid pool. This is due to the low values of the turbulent diffusivity in the lower part of the line and was verified by direct measurements of steel composition performed in the plant (Figure 8).

Consequently, the composition along the bar was calculated by convection of the elements concentration due to the casting speed and was considered homogeneous across the bar section.

D. *Final Calculations*

Having calibrated the model, a numerical code (GRADE[21]) was developed. The code calculates the dimensionless concentration $\tilde{C}(t)$ at the cut-off point of the bar, as a function of time.

The user is supposed to provide the following input data:

(1) casting speed as the piecewise function of time in each casting line;

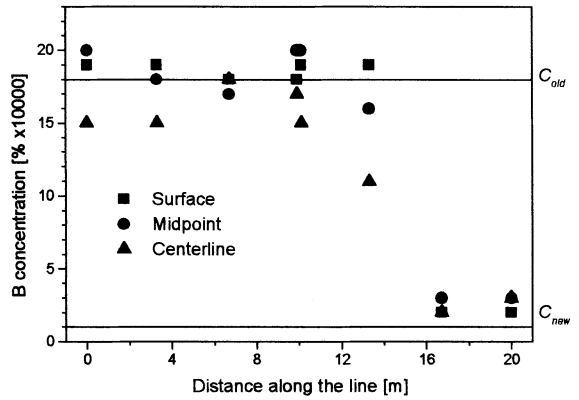

(*a*)

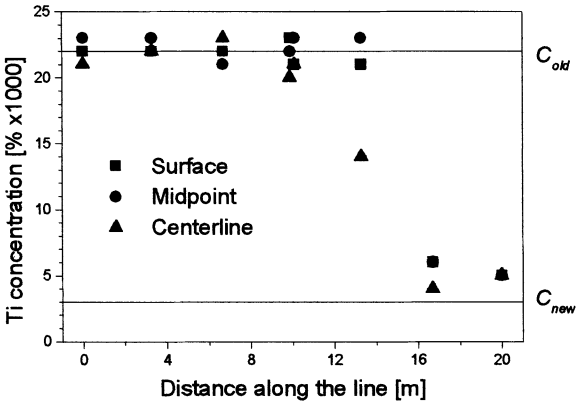

(*b*)

Fig. 8—(*a*) and (*b*) Experimental measurements along the downgraded bars (internal line) for different points of the bar cross section of example A.

(2) flow rate entering the tundish as the piecewise function of time;
(3) concentration of each element in the old and new grades;
(4) specification of the composition of both steel grades; and
(5) diameter of the bar.

With this information, the program is able to detect the old grade/intermixed steel boundary and the new grade/intermixed steel boundary in the bar at the cut-off point.

The program also calculates the proportion of new grade steel and old grade steel in the intermixed bar, which is needed to estimate the cost of the downgraded steel.

V. COMPARISON WITH PLANT MEASUREMENTS

The final validation of the model was accomplished by direct composition measurements of round billets from the Siderca S.A.I.C. continuous caster, performed with an optical emission in vacuum spectrometer. Typical precisions of these measurements are shown in Table II.

Two different changes of grade were analyzed, the first one having B and Ti as the critical elements and the second one having Cr and Mo as the critical elements.

In both cases, the filling of the tundish (after the drainage due to the ladle change) was performed in a double dilution process. This process is the standard procedure adopted by Siderca.

Table II. Experimental Precision in Chemical Composition Measurements in the Bars

Element	Units	Error
C	pct	0.012
Mn	pct	0.05
S	pct	0.001
P	pct	0.0016
Si	pct	0.015
Ni	pct	0.004
Cr	pct	0.025
Mo	pct	0.008
Sn	pct	0.001
Ti	pct	0.0002
Al	pct	0.005
B	pct	0.00002
Ca	pct	0.00015
Cu	pct	0.008

Table III. Casting Conditions of Example A

W_{tundish}	15.4 tons
W^1_{drain}	3.0 tons
W^1	6.0 tons
W^2_{drain}	4.0 tons
Q_{steady}	1.3 ton/min
Q^1_{dd}	3.05 ton/min
Q^2_{dd}	0.57 ton/min
Q^3_{dd}	3.56 ton/min
Bar diameter	0.170 m
Casting speed	2 m/min

A. *Plant Measurements—Example A*

The first set of measurements to be analyzed corresponds to a grade transition determined by the casting conditions of Table III and the chemical composition of Table IV.

In this case, B and Ti were the critical elements, since they were abundant in the old grade and had stringent restrictions for maximum concentration in the new grade. After casting two 10-meter-long bars of intermixed steel were downgraded on each line due to the high proportion of B and/or Ti.

Four samples were taken from each downgraded bar of an external line and from each downgraded bar of an internal line. The concentration of each element on these 16 samples was measured at the centerline, at the surface, and at a point placed between them. The resulting concentrations of Ti and B at different points of the bars are plotted on Figure 8. The figure shows that the differences in the composition of steel across the bar section are not important in determining the intermix region. This validates the assumption of negligible diffusion in the lower part of the line discussed in Section IV.

Figure 9 shows (for an external line) the concentration of different chemical elements, at the cut-off point, as a function of the length of steel bar cast since the moment of the new ladle first opening. The continuous lines are the results of the numerical model and the symbols represent experimental measurements. The good agreement observed indicates that the numerical model describes correctly the position and length of the intermixed bar.

In order to represent the deviation of our numerical results

Table IV. Chemical Composition of Example A

Element	Units	Old Grade			New Grade		
		Minimum	Maximum	Actual	Minimum	Maximum	Actual
C	pct	0.24	0.27	0.26	0.27	0.3	0.29
Mn	pct	1.3	1.45	1.33	1.25	1.4	1.31
S	pct	0	0.01	0.002	0	0.01	0.006
P	pct	0	0.025	0.016	0	0.02	0.019
Si	pct	0.25	0.35	0.29	0.3	0.4	0.36
Ni	pct	0	0.15	0.06	0	0.15	0.06
Cr	pct	0	0.2	0.03	0	0.16	0.05
Mo	pct	0	0.08	0.02	0	0.08	0.01
V	pct	0	0.01	0.003	0	0.01	0.002
Nb	pct	0	0.005	0.001	0	0.005	0.001
Ti	pct	0.015	0.035	0.022	0	0.014	0.003
Al	pct	0.01	0.035	0.021	0.01	0.03	0.018
B	pct	0.0015	0.0025	0.0018	0	0.0005	0.0001
N	pct	0	0.009	0.0048	0	0.009	0.004
Ca	pct	0	0.01	0.0013	0	0.01	0.0017
Cu	pct	0	0.22	0.14	0	0.25	0.17

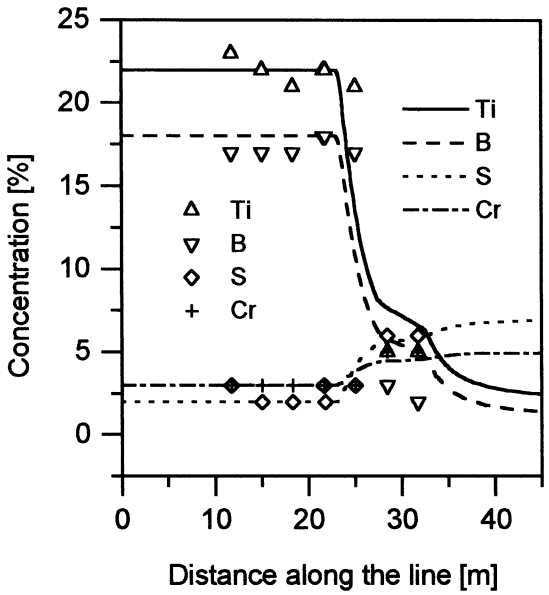

Fig. 9—Numerical results (lines) and plant measurements (symbols) of chemical composition for external line downgraded bars. Four elements were considered: Ti (1000 times), B (10,000 times), S (1000 times), and Cr (100 times).

from the experimental data, the following parameter is defined:

$$\delta^{(e)} = \frac{\sqrt{\sum_{i=1}^{N} (C^{(e)}_{Exp,i} - C^{(e)}_{Num,i})^2}}{\sqrt{\sum_{i=1}^{N} (C^{(e)}_{Exp,i})^2}} \qquad [6]$$

where $C^{(e)}_{Exp,i}$ and $C^{(e)}_{Num,i}$ are concentrations of the chemical element (e) at different positions of the bar, as given by experimental measurements and numerical model, respectively; and N is the total number of measurements.

For the critical elements of this example, we obtained $\delta^{(B)} = 0.182$ and $\delta^{(Ti)} = 0.162$. These values were calculated considering surface, midpoint, and centerline measurements of concentrations.

Table V. Casting Conditions of Example B

$W_{tundish}$	13.0 tons
W^1_{drain}	5.1 tons
W^1	7.3 tons
W^2_{drain}	5.3 tons
Q_{steady}	1.0 ton/min
Q^1_{dd}	2.9 ton/min
Q^2_{dd}	0.1 ton/min
Q^3_{dd}	3.5 ton/min
Bar diameter	0.148 m
Casting speed	2 m/min

B. *Plant Measurements—Example B*

The second grade change analyzed is described by Tables V and VI and corresponds to a much longer intermix (six bars were downgraded on each line). Again, four samples were taken from each downgraded bar of an external line and of an internal line. This time, however, only one measurement was performed on each sample. This measurement was taken after forging the samples, which is the usual procedure carried out in plants to measure steel composition. Thus, the measured concentration is, in fact, an average of its value across the bar section. In this case, Cr and Mo were the more critical elements.

Figure 10 shows the numerical results (lines) and the experimental points (symbols) for four different chemical species on the intermixed steel bars. The figure shows that the model is able not only to make a good estimation of the position and length of the intermixed bars, but also to describe accurately the concentration profile along the bars. Even the concentration plateau, due to the ladle closing during the double dilution process, was successfully reproduced.

In order to represent the deviation of our numerical results from the experimental data, the $\delta^{(e)}$ parameter (Eq. [6]) is calculated for the critical elements: $\delta^{(Cr)} = 0.076$ and $\delta^{(Mo)} = 0.079$. In this example, measurements were carried out after forging the samples.

Table VI. Chemical Composition of Example B

		Old Grade		New Grade			
Element	Units	Minimum	Maximum	Actual	Minimum	Maximum	Actual
C	pct	0.09	0.13	0.12	0.11	0.14	0.13
Mn	pct	0.4	0.5	0.46	1	1.15	1.03
S	pct	0	0.01	0.001	0	0.005	0.005
P	pct	0	0.015	0.01	0	0.02	0.012
Si	pct	0.12	0.23	0.17	0.3	0.4	0.32
Ni	pct	0	0.15	0	0	0.15	0.0
Cr	pct	2.03	2.13	2.11	0	0.16	0.11
Mo	pct	0.92	0.97	0.94	0	0.08	0.01
V	pct	0	0.01	0.005	0	0.01	0.001
Nb	pct	0	0.005	0.004	0	0.005	0.001
Ti	pct	0	0.005	0.002	0	0.005	0.004
Al	pct	0.01	0.035	0.023	0.015	0.04	0.028
B	pct	0	0.0005	0.0001	0	0.0005	0.0001
N	pct	0	0.01	0.0057	0	0.008	0.0048
Ca	pct	0	0.01	0.0024	0	0.01	0.0016
Cu	pct	0	0.15	0.006	0	0.2	0.16

VI. TUNDISH FILLING PROCEDURES

To illustrate the advantage of filling the tundish by the double dilution procedure, example B in the previous section is going to be considered again together with a simple dilution procedure example.

In Section V–B, a double dilution procedure was simulated with parameters of Table V given by real casting conditions. Now, the same grade change (shown in Table VI) will be simulated with a simple dilution procedure (Table VII).

Figure 11 shows the concentration of Cr along the bar as calculated by simulating simple dilution and double dilution procedures. The advantage of the double dilution procedure becomes evident since its curve reaches the critical concentration before the simple dilution curve does. In this example, 9 m of steel bars are saved on each internal line and 7 m on each external line when a double dilution procedure is used. A total amount of 4 tons of steel was saved.

VII. MODEL EXTENSION

The model was employed in a particular configuration of a four line round billet caster and it can simulate different conditions on

(1) casting speed,
(2) minimum level of the liquid metal maintained in the tundish,
(3) flow rate entering the tundish
(4) dilution strategies (simple, double, or other type of dilution)
(5) grades being cast, and
(6) casting sequence.

A new calibration needs to be performed any time the configuration of the caster is changed, for example, due to changes in the size or shape of the tundish, changes in the flow control devices in the tundish, or changes in the diameter of the mold.

The model can be extended to include casters with any number of lines (not necessarily symmetric) by adding a group of volumes associated to each line in the tundish model, according to Figure 12. In order to allow the recirculation of fluid among the groups of volume, a connecting mixing volume must be added, according to Figure 13.

The model can also be applied to slab casters or billet casters. However, diffusive effects in the third submodel can not be negligible and additional calculations must be carried out to get the final composition of the slab or billet.

VIII. CONCLUSIONS

The grade transition process in the round billets continuous caster of Siderca was studied and a numerical model was developed. The model provides a fast and accurate estimation of the position and length of the steel bar to be downgraded. The main conclusions of this study are as follows.

1. A methodology to model the mixing in the tundish with several continuous casting lines is presented, in which a defined group of volumes is associated with each line. Mixing volumes connect the different groups to allow recirculation of fluid.
2. The model can simulate different casting conditions including time-dependent casting speed and flow rate entering the tundish. In particular, the filling of the tundish in two consecutive steps ("double dilution" process) was successfully simulated.
3. The double dilution process was found to be more efficient to evacuate the old grade steel remaining in the tundish compared with the simple dilution process.
4. The short running times and the user friendly interface allows the program to be used practically on line in the plant, to indicate where the bars must be cut and to find the optimal sequence of steel grades to be cast.
5. Most of the steel mixing takes place in the tundish. This is probably due to the relatively small volume of liquid steel present in each casting line of the modeled cases, whose diameters are 0.148 or 0.170 m. Both numerical calculations and measurements show that diffusion effects can be neglected in most part of the bar.
6. The low values of the deviation parameter $\delta^{(e)}$ (defined by Eq. [6]) show the good agreement between the numerical

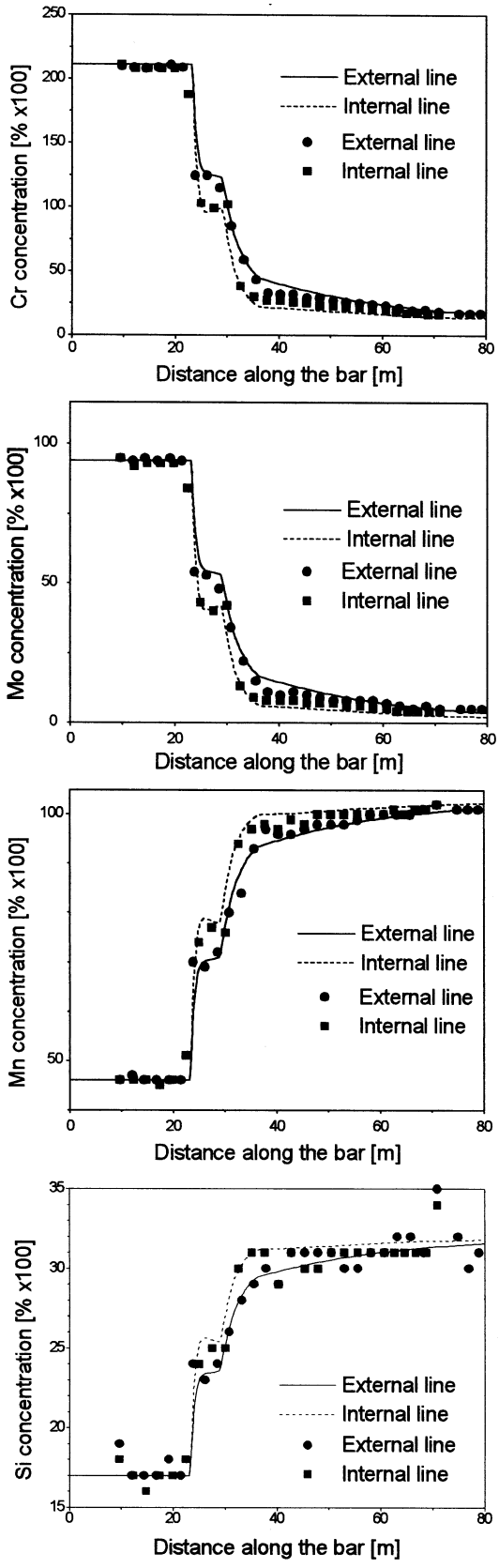

Fig. 10—Numerical results (lines) compared with plant measurements (symbols) for four different chemical elements of example B.

Table VII. Casting Conditions of Simple Dilution

W_{tundish}	13.0 tons
W^1_{drain}	5.1 tons
Q_{steady}	1.0 ton/min
Q_{sd}	3.5 ton/min
Bar diameter	0.148 m
Casting speed	2 m/min

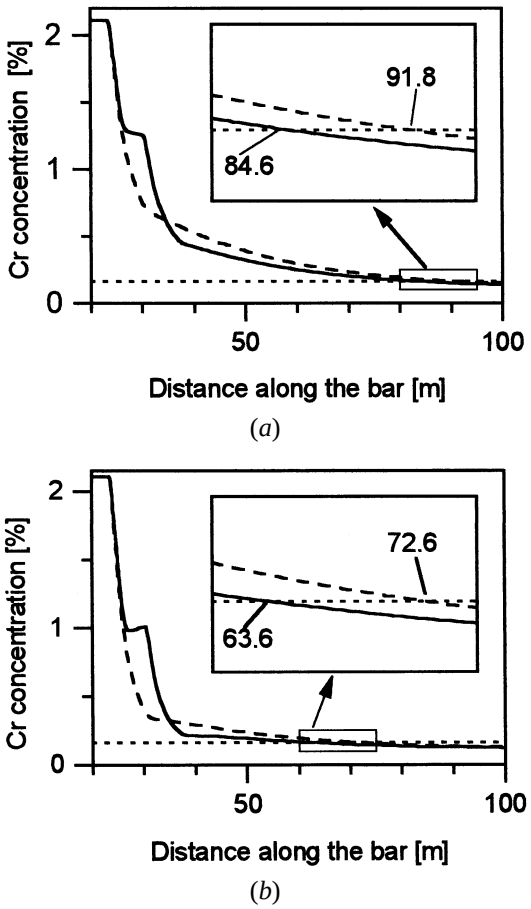

Fig. 11—(*a*) and (*b*) Concentration of Cr along the bar for the grade transition given by Table VI. The figure compares results obtained with the simple dilution process (dashed line) and double dilution process (full line). The dotted line represents the maximum concentration of Cr allowed in the new grade.

results and the measurements carried out in a round billet caster.

LIST OF SYMBOLS

C	actual concentration of any chemical element
$\tilde{C}$	actual dimensionless concentration of any chemical element.
$\hat{C}$	dimensionless concentration in RTD curves.
C_i^j	concentration of any chemical element at the exit of volume V_i^j
$C^{(e)}_{\text{Exp},i}$	measured concentration of chemical element (e)
$C^{(e)}_{\text{Num},i}$	numerical concentrations of chemical element (e)
D_{eff}	effective diffusivity.

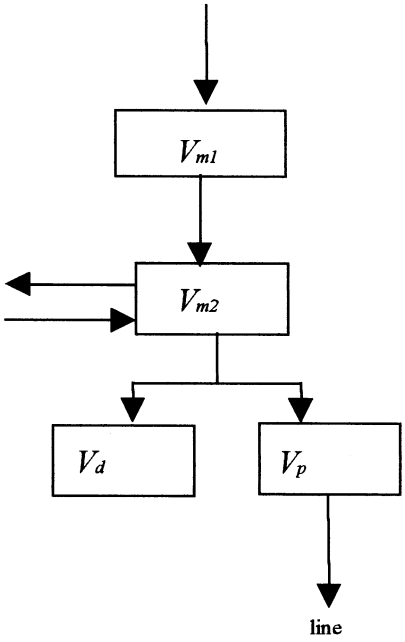

Fig. 12—Group of volumes associated to each line.

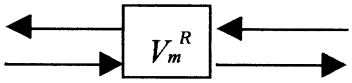

Fig. 13—Mixing volume connecting groups associated to different lines.

D	molecular diffusivity
D^t	turbulent diffusivity
f_i	fraction of the volume i
N	total number of measurements in Eq. [6].
Q	flow rate
Q_i	flow rate between different volumes of the model
t	time
t_p	time delay introduced by plug flow volumes.
$\hat{t}$	dimensionless time
V	volume
v	casting speed
x_i	flow rate fraction
z	distance to the meniscus, measured along the bar
z_i	beginning of the diffusion-convection region
z_f	end of the diffusion-convection region

Greek Symbols

δ	deviation parameter
μ^t	turbulent viscosity
ρ	steel density
ϕ	bar diameter

Superscripts

(e)	chemical element
en	entering the tundish
ext	external line
int	internal line
R	recirculating

Subscripts

d	dead
exp	experimental
m	mixing
new	new
num	numerical
old	old
p	plug

ACKNOWLEDGMENTS

The authors thank Dr. E. Dvorkin for his continuous support regarding the numerical methods. This research was supported by SIDERCA S.A.I.C. (Campana, Argentina)

REFERENCES

1. M.T. Burns, J. Schade, W.A. Brown, and K.R. Minor: *Iron Steelmaker*, 1992, pp. 35-39.
2. X. Huang and B. Thomas: *Metall. Mater. Trans. B*, 1993, vol. 24, pp. 379-93.
3. X. Huang and B. Thomas: *Metall. Mater. Trans. B*, 1996, vol. 27B, pp. 617-32.
4. H. Chen and R. Pehlke: *Metall. Mater. Trans. B*, 1996, vol. 27B, pp. 745-56.
5. J. Watson, H. Huang, and B. Thomas: *Steel Technol. Int.*, 1996, pp. 165-70.
6. B.G. Thomas: *Steelmaking Conf. Proc.*, Pittsburgh, PA, Iron and Steel Society, Warrendale, PA, 1996, pp. 519-31.
7. F. Ors, G. Alvarez de Toledo, O. Caballero, E. Lainez, and J. Laraudogoitia: *3rd Eur. Conf. on Continuous Casting*, Madrid, Spain, Unesid, Madrid, Spain, 1998.
8. F.J. Mannion, A. Vassilicos, and J.H. Gallenstein: *75th Steelmaking Conf. Proc.*, 1992, vol. 10, pp. 177-86.
9. M.C. Tsai and M.J. Green: *74th Steelmaking Conf. Proc.*, 1991, pp. 501-04.
10. A. Diener, E. Görl, W. Pluschkell, and K.D. Sardemann: *Steel Res.*, 1990, vol. 61 (10), pp. 449-54.
11. D. Martin, M. Ferreyra, J. Madias, A. Campos, G. Walter, E. Rey, E. Guastella, and A. Garamendy: "Estudio en Modelo de Agua del Flujo de Acero en el Repartidor de la Máquina 2 de SIDERCA," IAS Report, IAS, San Nicolás, Argentina, 1997 (in Spanish).
12. M.B. Goldschmit and M.A. Cavaliere: *Appl. Mech. Rev.*, 1995, vol. 48 (11).
13. M.B. Goldschmit and M.A. Cavaliere: *Eng. Comput.*, 1997, vol. 14, pp. 441-55.
14. M.B. Goldschmit and R. Javier Principe: *IV World Congr. on Computational Mechanics*, Buenos Aires, Argentina, 1998.
15. M.B. Goldschmit, R.J. Príncipe, and M. Koslowski: *3rd Eur. Conf. on Continuous Casting*, Madrid, 1998.
16. M.B. Goldschmit, R.J. Príncipe, and M. Koslowski: *Int. J. Num. Methods in Eng.*, 1999, vol. 46, pp. 1505-19.
17. *FANTOM, User manual*, International Center for Numerical Methods in Engineering, Universitat Politècnica de Calalunya, Barcelona, Spain, 1994.
18. T.J.R. Hughes and A. Brooks: *Finite Element in Fluids*, 1982, pp. 47-65.
19. A. Brooks and T.J.R. Hughes: *Computer Methods App. Mech. Eng.*, 1982, vol. 32, pp. 199-259.
20. O.C. Zienkiewicz and R.L. Taylor: *The Finite Element Method*, 4th ed., McGraw-Hill, London, 1989.
21. *GRADE, User Manual*, Center for Industrial Research, FUDETEC, Argentina, 1999.